Anat Sci Int (2009) 84:226–236
DOI 10.1007/s12565-009-0028-z

ORIGINAL ARTICLE

Role of the CXCL12/CXCR4 axis in milky spots of rats bearing ascitic-type hepatoma

Hirokazu Abe · Keisuke Ina · Hirokazu Kitamura · Hideaki Sumiyoshi · Shuji Tatsukawa · Hidekatsu Yoshioka · Yoshihisa Fujikura

Received: 8 May 2008 / Accepted: 23 December 2008 / Published online: 2 April 2009

Abstract Rat ascitic-type hepatoma AH7974 cells express CXCR4 mRNA and protein at high levels and also show vigorous migratory responses to its ligand CXCL12. We have shown that AMD3100 (a specific CXCR4 antagonist) effectively reduced tumor invasion into the milky spot in Sprague–Dawley rats inoculated with AH7974 cells. A histological analysis revealed that the milky spots from AMD3100-treated rats were both smaller and consisted of fewer constituent cells and blood vessels than those from the AH7974 inoculated rats. Alkaline phosphatase staining also showed a statistically significant reduction in the area of the milky spots in the AMD3100-treated rats in comparison to the AH7974 inoculated rats ($P < 0.0001$). Green fluorescence protein (GFP)-tagged AH7974 cells were constructed to detect the localization of the tumor cells in the milky spots. There were fewer GFP-tagged AH7974 cells in the AMD3100-treated rats than in the AH7974 inoculated rats. The number of eosinophils and mast cells increased in the milky spots of AH7974-inoculated rats, and angiogenesis was also seen. In comparison, both cell proliferation and angiogenesis were inhibited in the milky spots of the AMD3100-treated rats. Collectively, our results strongly suggest that the CXCR4/CXCL12 axis plays an important role in the development of peritoneal carcinomatosis. As such, CXCR4 may be a potential therapeutic target for peritoneal carcinomatosis.

H. Abe · K. Ina · H. Kitamura · H. Sumiyoshi · S. Tatsukawa · H. Yoshioka · Y. Fujikura (✉)
Department of Anatomy, Biology and Medicine,
Faculty of Medicine, Oita University,
1-1 Idaigaoka, Hasama-machi, Yufu,
Oita 879-5593, Japan
e-mail: ham8@med.oita-u.ac.jp

Keywords AH7974 · AMD3100 · CXCL12 · CXCR4 · Milky spot

Introduction

The presence of milky spots in the human greater omentum was first reported by Seifert (1921) 88 years ago. These milky spots appear as tiny, cotton wool-like masses that are fairly difficult to identify by the naked eye. They are usually embedded in adipose tissue, particularly in preserved specimens, but they can be found in other areas of the peritoneum (Shimotsuma et al. 1991). These omental milky spots mainly consist of macrophages, lymphocytes, and blood vessels in the form of blood capillaries with a glomerular shape (Shimotsuma et al. 1991). The dilation and increased number of these capillaries lead to the migration of macrophages and lymphocytes from the blood vessels into the milky spots, a process that enhances the immune function of the latter (Shimotsuma et al. 1992; Krist et al. 1995). The cell population in the milky spot was found to comprise 47.5% macrophages, 29.1% B-lymphocytes, 11.7% T-lymphocytes, and 6.1% mast cells, with lymphocytes primarily inside the milky spots, many macrophages in the outer layer, and mast cells situated along the capillary vessels (Shimotsuma et al. 1991). As an entity, the milky spot, which is lymphoid tissue on the peritoneum, is considered to be a gate through which small particles are absorbed from the peritoneal cavity into the subperitoneum (Higgins and Bain 1930).

The greater omentum covers the gastrointestinal tract. It prevents the diffusion of inflammation, but it is also the first site of metastasis for most abdominal tumors (Green and Williams 1978). Digestive tract cancers readily metastasize to the greater omentum, and the milky spots

appear to be the target site (Higgins and Bain 1930). As such, they may contribute to the peritoneal spreading of cancer cells. An omentectomy has been shown to prolong the survival time of patients (Lawrance et al. 1991) and animals at very early stages of peritoneal carcinomatosis (Yoshie et al. 1997).

The expression of chemokine receptors, especially CXCR4, by tumor cells can be an important factor in organ-specific metastases (Jones et al. 2000; Rempel et al. 2000; Geminder et al. 2001; Murphy 2001; Strieter 2001; Taichman et al. 2002). Mashino et al. (2002), for example, reported that tumor cells from the breast expressed CXCR4, whereas high concentrations of CXCL12 (also called stromal-derived factor-1α) were present at the common site of metastasis of prostate cancer. The interaction between CXCL12 and its specific receptor CXCR4 has also been implicated in the bone metastasis of prostate cancer (Taichman et al. 2002). Furthermore, the CXCL12/CXCR4 axis has been shown to be involved in the metastasis of non-small-cell lung cancer cells, particularly in their dissemination into the pleural space (Oonakahara et al. 2004). CXCR4 is widely expressed on different cell types, including B cells, T cells, blood vessel endothelial cells, and dendritic cells (Nagasawa et al. 1999) involved in chemotaxis. CXCL12 is rather unique among chemokines in that it recognizes only a single receptor (CXCR4), which, itself, is only recognized by CXCL12 (Clercq et al. 1992; Oberlin et al. 1996; Rossi and Zlotnik 2000). This chemokine is expressed in almost all organs, and it is widely held that the tissue stroma cell mainly expresses CXCL12 constitutively. CXCL12 is characterized by being able to develop constitutively, whereas many chemokines develop due to the stimulation of inflammation (Oberlin et al. 1996). However, the control of CXCL12 expression remains unknown. It has been reported that CXCL12 contributes to cell migration activity for many cell strains, including lymphocytes, blood precursor cells, and blood vessel endothelial cells (Bleul et al. 1996; Oberlin et al. 1996; Nagasawa et al. 1999; Egawa et al. 2001), and it is known to promote the survival of several cell types, including lymphocytes and blood precursor cells (Nagasawa et al. 1994, 1999; Nanki and Lipsky 2000; Egawa et al. 2001).

The rat ascitic-type hepatoma cells, named AH7974, were originally induced by Yoshida (1971). These tumor cells are particularly stable and easy to treat in comparison to other ascitic-typed hepatomas.

CXCR4 acts as a receptor on the surface of the host cell of human immunodeficiency virus-1 (HIV-1), and it is also an essential molecule for the onset of acquired immune deficiency syndrome (AIDS). AMD3100 is the most active member of the bicyclam family of compounds while other, less potent, congeners differ solely in their linkage bridging the two cyclam subunits (Clercq et al. 1992). The bicyclams were originally synthesized as part of a program to develop HIV inhibitors; they were found to inhibit HIV-1 and HIV-2 infection at an early stage of the viral life cycle, before reverse transcription was inhibited (Clercq et al. 1992, 1994; Vreese et al. 1996a, b). AMD3100 selectively antagonizes CXCR4 (Feng et al. 1996; Nagasawa et al. 1999), which acts as a corecepter for HIV (Shiomi et al. 2006), and inhibits the in vitro chemotactic and intracellular Ca^{2+} flux response of human monocytes to CXCL12 (Feng et al. 1996). These characteristics make AMD3100 an ideal tool to evaluate the physiological and pathological importance of the CXCL12/CXCR4 interactions. The role of the CXCR4/CXCL12 axis of the tumor cell in the milky spot has not yet been studied.

We report here the results of our study of the mechanism by which the intraperitoneal tumor cells invade the milky spots, using histological and biochemical methods. Our aim was to establish a new treatment method for preventing peritoneal metastasis by focusing on the chemotaxis of the tumor cells.

Materials and methods

Animals

Specific, pathogen-free, 6- to 8-week-old male Sprague–Dawley (SD) rats were obtained from Kyudo (Tosu, Japan). The animals were quarantined for 1 week under pathogen-free conditions to confirm the absence of diseases before use. The Oita University Guidelines for the Care and Use of Laboratory Animals based on the National Institutes of Health Guide for the Care and Use of Laboratory Animals (National Academies Press, Washington D.C.) were applied for all experiments using these rats.

The rats were divided into three experimental groups: (1) the control animals (CONT) were injected with physiological saline and killed 3 days later; (2) the AH rats were administered AH7974 tumor cells intraperitoneally (i.p.) and killed 3 days later; (3) the AMD rats were inoculated with AH7974 cells and 2.5 mg AMD3100 (Sigma, St. Louis, MO) on experimental day 0 and then inoculated with 2.5 mg AMD3100 again on the following two days; the rats were killed on the third experimental day. The AH7974 cells that were injected into the AH and AMD rats were adjusted to provide 1×10^7 cells/ml of saline solution, and they were rapidly disseminated in the abdominal cavities of the rats following the i.p. inoculation.

Cell line

The rat ascitic-type hepatoma cell line, AH7974, was used for this experiment. The cell line was maintained in RPMI

1640 medium supplemented with 10% fetal bovine serum (FBS) and 50 mg/ml gentamicin (Schering-Plough, Osaka, Japan) in a CO_2 incubator.

Alkaline phosphatase staining

Alkaline phosphatase (ALPase) stains the endothelial cells of capillaries and arterioles to a violet color. The greater omentum removed from each of the sacrificed animals was fixed by immersion in 4% paraformaldehyde for 90 min and rinsed three times, 10 min each time, by immersion in 0.1 *M* cacodylate buffer (pH 7.2). It was then incubated in the reaction medium for ALPase activity determination according to the azo-dye method (Kato et al. 1993). In brief, the medium contains 80 mg naphthol AS-MX phosphate disodium salt (Sigma) dissolved in 4 ml *N*,*N*′-dimethyl-formamide and 80 mg fast blue BB salt (Sigma) dissolved in 80 ml 0.1 *M* Tris–HCl buffer (pH 8.5). The organ was incubated in this medium for 30 min at 4°C, rinsed by immersion in distilled water several times, and photographed on a stereoscope (Olympus, Tokyo, Japan). The milky spot is oval in shape, and we used a special formula to measure and subsequently calculate the area of each milky spot from the photographs. If the length of the vertical axis of the milky spot is "*a*", and the length of the cross axis of the milky spot is "*b*", the area of milky spot "*S*" will be expressed as $S = \pi ab/4$.

Immunocytochemistry

Indirect immunocytochemistry was performed for either CXCR4 or CXCL12 on the AH7974 cells. The cells were non-fixed and incubated with rabbit anti-rat CXCR4 polyclonal antibody (Abcam, Cambridge, UK) or rabbit anti-rat CXCL12 antibody (GeneTex, San Antonio, TX) for 2 h at room temperature (RT), followed by three rinses of the sections with 0.1 *M* phosphate buffered saline (pH 7.2, PBS), incubation with a 1:40 dilution of goat anti-rabbit FITC conjugated immunoglobulin (Ig)G (Wako, Osaka, Japan) for 1 h at RT and, finally, another three rinses in PBS. After staining, the cells were observed and photographed using an Olympus BX 60 microscope equipped with epifluorescence optics.

Immunohistochemistry

The surgical specimens from the greater omentum were fixed in 4% paraformaldehyde in 0.1 *M* cacodylate buffer for 2 h. The tissue was dehydrated in a graded series of ethanol and embedded in paraffin. Consecutive sections were cut to a 5-μm thickness. The sections were evaluated by indirect immunogold-silver staining (Kitamura et al. 1991) to determine the pattern of CXCL12 and CXCR4 expression in the milky spots. In brief, the sections were first reacted with the primary antibody, rabbit anti-rat CXCR4 polyclonal antibody, or rabbit anti-rat CXCL12 polyclonal antibody, for 2 h at RT. The sections were then rinsed in PBS and further incubated with the gold-labeled secondary antibody, goat anti-rabbit IgG-gold (5 nm) (Amersham Biosciences, Buckinghamshire, UK), for 1 h at RT. The sections were finally developed for 28 min at 23°C with the developer, which contained 0.02% 18-crown-6 (Sigma-Aldrich, St. Louis, MO), 0.17% hydroquinone, and 0.17% silver nitrate in 0.2 *M* citrate buffer (pH 3.45). The reaction was recognized as a black color. The immunolabeled sections were observed and photographed.

Transmission electron microscopy

The animals were anesthetized with Nembutal and exsanguinated from a common carotid artery, following which the greater omentum was removed for the histological evaluation. The organ was immersion-fixed in twofold diluted Karnovsky's fixative for 2 h at 4°C, then washed and immersed in 0.1 *M* cacodylate buffer (pH 7.4) overnight at 4°C. The specimen was post-fixed in 2% osmium tetroxide–1% potassium ferrocyanide for 2 h at 4°C, dehydrated in an ascending series of ethanol, and finally embedded in epoxy resin. Ultrathin sections were cut on an ultramicrotome (LKB2088 Ultrotom V, Bromma, Sweden), mounted on copper grids, and stained with methanolic uranyl acetate and lead citrate. The section was observed and photographed under transmission electron microscopy (TEM; model 1200EX II; JEOL, Tokyo, Japan) at a pressure of 80 kV. To clarify the ultrastructural features of the AH7974 cells, we also immersion-fixed AH7974 cell pellets in twofold diluted Karnovsky's fixative for 2 h at 4°C and then examined them by TEM.

Western blot analysis

The cells were cultured in RPMI 1640 medium supplemented with 10% FBS. The cell lysates were prepared with sample buffer [25 mmol/l Tris–HCl, pH 6.8, 5% w/v glycerol, 1% w/v sodium dodecyl sulfate (SDS), 0.05% w/v bromophenol blue], subjected to SDS-polyacyrlamide gel electrophoresis (PAGE), and transferred to Immobilon-P membranes (Millipore, Bedford, MA). The blots were probed by the primary antibodies and then rinsed in 0.1 *M* phosphate buffer (pH 7.4) and further incubated for 1 h at RT with the gold-labeled secondary antibody. The blots were finally developed for 28 min at 23°C. The same developer as that used in the immunohistochemistry method was prepared. The immunolabeled blots were observed and photographed.

Table 1 Primer sequences used in the reverse transcriptase-PCR analysis of rat chemokine receptors

Gene	Primers
CXCR4	5′-ATCTTCCTGCCCACCATCTATTTTATCATC-3″ (forward)
	5′-ATCCAGACACCCACATAGACGGCCTTTTCA-3″ (reverse)
CXCL12	5′-CCGCGCTCTGCATCAGTGACGGTAAG-3″ (forward)
	5′-CTTGTTTAAGGCTTTGTCCAGGTACT-3″ (reverse)
GAPDH	5′-CTACCCACGGCAAGTTCAACGGCA-3″ (forward)
	5′-TCCAGGCGGCATGTCAGATCCACA-3″ (reverse)

RNA preparation and reverse transcription-PCR

Total RNA was isolated from the AH7974 cell pellets using acid guanidium thiocyanate and phenol–chloroform, and 2-μg samples were reverse-transcribed in 50 μl of reaction mixture containing reverse transcription buffer, 10 m*M* dithiothreitol, 1 m*M* of each dNTP, 50 ng of random hexamers, 100 U RNase inhibitor, and 200 U MMLV reverse transcriptase (Invitrogen, Carlsbad, CA) at 37°C for 2 h. A reverse transcription-PCR (RT-PCR) was performed using the primer sequences shown in Table 1. The PCR products were resolved electrophoretically on a 1.2% agarose gel, and the gel was stained with ethidium bromide and photographed under UV light.

Stable transfection of the green fluorescence protein expression vector

The green fluorescence protein (GFP) stable expression vector pEGFP-C3 (Clontech, Palo Alto, CA) contains a neomycin resistance gene. The constructs were transfected into the AH7974 cells, and the stable transformed cells were selected at a G418 final concentration of 500 μg/ml.

Statistical analysis

The data are presented as the mean ± standard deviation (SD). The analysis of the results was performed using the unpaired Student's *t* test. A value of $P < 0.05$ was considered to be significant.

Results

Morphological characterization of the AH7974 cells

The shape of the AH7974 cells were round or oval, and they displayed polychromasia (Fig. 1).

Visualization of milky spots by ALPase staining of the rat greater omentum

The milky spots were stained by ALPase, which enabled visualization stereoscopically. At a high magnification, we were able to confirm that many blood capillaries and arterioles formed a glomerulus-like network in the milky spot (data not shown).

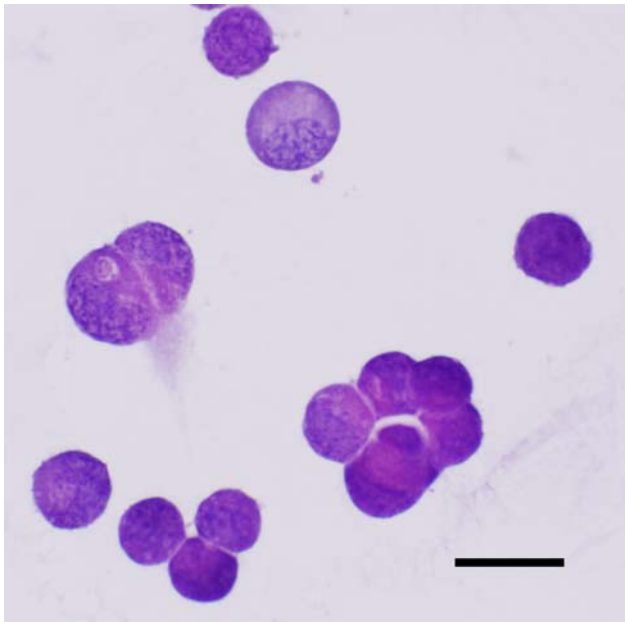

Fig. 1 Morphological images of the AH7974 cells stained with hematoxylin and eosin. *Scale bar*: 30 μm

In the greater omentum of the CONT rats, several milky spots were present on both sides of the omental branches, which consistently ramified from the gastroepiploic artery. (Fig. 2a).

During the experimental period, the size of the milky spots in the omenta of the AH rats increased relative to those of the CONT rats (Fig. 2b).

The milky spots in the greater omenta of the AMD rats were smaller than those observed in the greater omenta of the AH rats, and the shape of the milky spot in the former became more slender in the border area (Fig. 2c).

Comparison of the area of the milky spot

We randomly photographed 76 fields of vision (FOV) in the CONT rats, 216 FOV in the AH rats, and 181 FOV in the AMD rats and then measured the areas of the 889 milky spots visualized in the CONT rats, 2710 milky spots visualized in the AH rats, and 2025 milky spots visualized

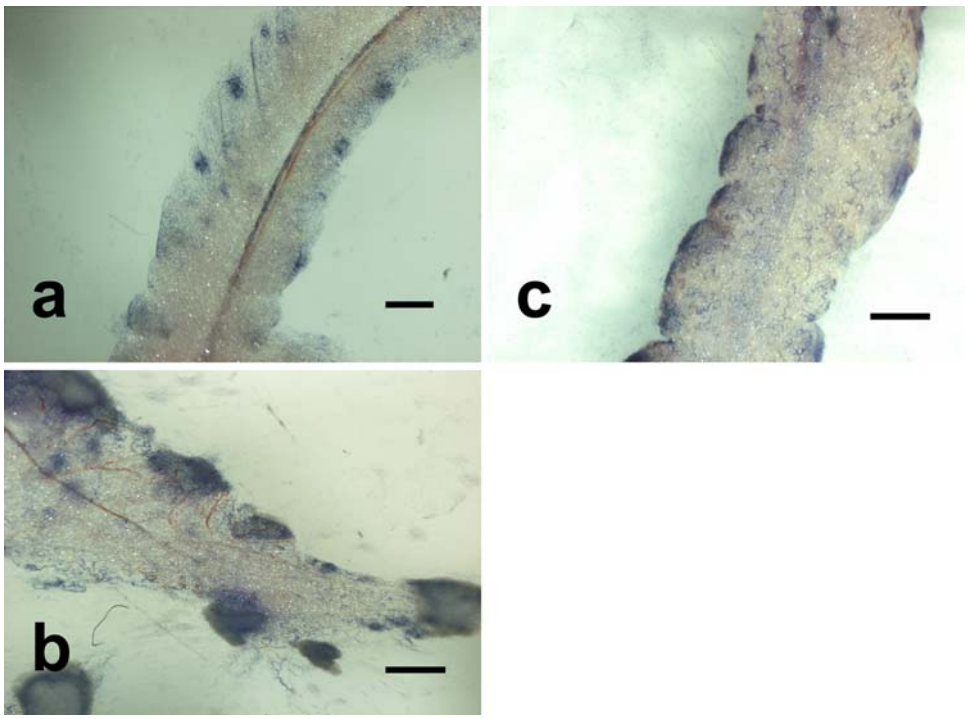

Fig. 2 Alkaline phosphatase (ALPase) staining of the greater omentum from a control rat (CONT; **a**), an AH rat (AH7974 tumor cells administered intraperitoneally;**b**), and an AMD rat (inoculated on day 0 with AH7974 cells and 2.5 mg AMD3100 and on the following 2 days with 2.5 mg AMD3100; **c**). The *dark-blue areas* are the milky spots. The spots from the AH rats can be seen to be larger than those from the other groups. *Scale bars*: 1 mm

in the AMD rats. We subsequently calculated the average area and SD for each group. The average area of the milky spots from the AH rats was significantly larger than that of the CONT rats (12.672 ± 1.039 vs. 12.120 ± 0.801 μm^2, respectively; $P < 0.001$). The average area of the spots visualized in the AMD rats was significantly reduced in comparison to that of the AH rats (12.218 ± 0.630 vs. 12.672 ± 1.039, respectively; $P < 0.001$) (Fig. 3).

Selective expression of CXCR4 in AH7974 cell line

The AH7974 cell line clearly expressed CXCR4 mRNA (Fig. 4a). mRNA expression of CXCL12 in the AH7974 cell line was also examined but the mRNA could not be recognized.

Protein expression of CXCR4 was also examined by Western blot (Fig. 4b) and immunocytochemistry using a specific antibody. CXCR4 protein bands were recognized at about 39 and 78 kDa (Fig. 4b), with the 39-kDa corresponding to CXCR4 and the 78-kDa band being the dimmer of CXCR4. The protein was localized on the cell surface and/or in the cytoplasm of the AH7974 cells (Fig. 4c). The AH7974 cells produced CXCR4 protein, but not CXCL12 protein (data not shown).

Histological organization of the milky spots

The milky spots of the CONT rats had only a few constituent cells and only a few blood vessels (Fig. 5a, b), with

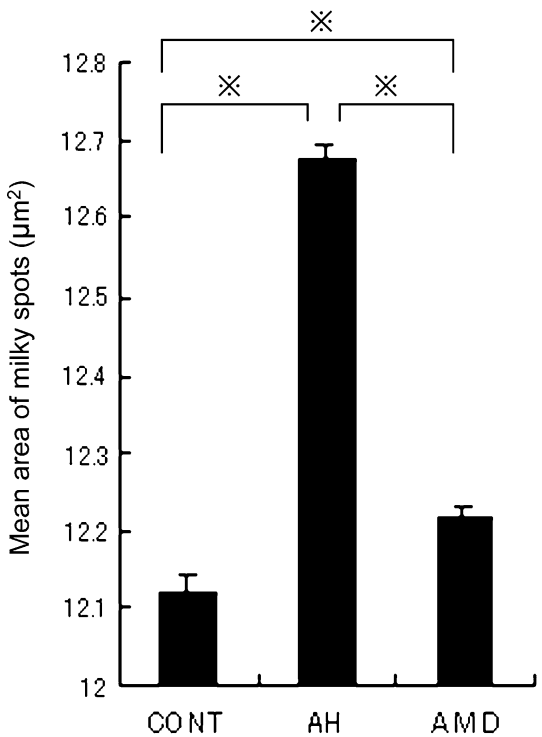

Fig. 3 Comparison of the mean area of the milky spots in the three groups of rats (for explanation of groups, see caption to Fig. 2 and "Methods and materials", subsection "Animals"). The mean area of the milky spots visualized in the AH rats was greater than that from the other groups. *Vertical axis* A log conversion was performed to simplify the comparisons. Values are the mean ± standard deviation (SD). ※ $P < 0.001$

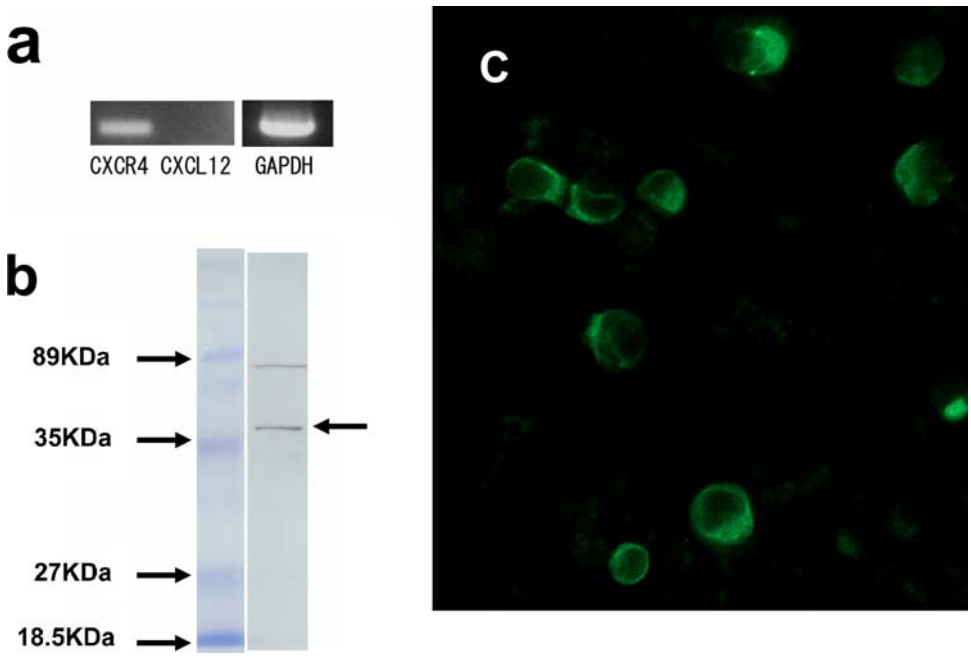

Fig. 4 Reverse transcriptase-PCR (RT-PCR) analysis, Western blot analysis, and immunocytochemical staining for the expression of CXCR4 in the AH7974 cells. **a** RT-PCR analysis of the expression of CXCR4 and CXCL12 in the AH7974 cells. *GAPDH* Glyceraldehyde-3-phosphate dehydrogenase. **b** Western blot analysis using anti-CXCR4 antibody against the AH7974 cell lysates; two bands (approx. 39 and 78 kDa) are clearly recognizable on the membrane. **c** Immunocytochemical analysis using anti-CXCR4 antibody on the AH7974 cells. CXCR4 protein is expressed at least on the cell surface of the AH7974 cells

lymphocytes and, on a smaller scale. eosinophils and macrophages present in milky spots. Mesothelial cells were visible on the surface of the milky spot from the CONT rats. In the milky spots from the AH rats, the number of cells constituting the milky spots had increased relative to those of the CONT rats, as had the size (Fig. 5c, d), as revealed by the serial sections. Enlarged blood vessels were conspicuous in the milky spots from AH rats (Fig. 5c), and eosinophils and tumor cells that had invaded the spot were recognizable (Fig. 5d).

The size of the milky spots of the AMD rats markedly decreased in comparison to those of the AH group (Fig. 5e, f). The number of cells in the spots, including the eosinophils, as well as of blood vessels also decreased.

Immunohistochemical analysis using anti-CXCL12 and anti-CXCR4 anti-bodies

In the section of the milky spots from the CONT rats, CXCR4 was recognized on/in the red blood cells (Fig. 6-1b), while CXCL12 protein was not recognized on/in the mesothelial cells, red blood cells, or blood endothelial cells (Fig. 6-1c).

In the section of the spots from the AMD rats, neither CXCR4 nor CXCL12 was barely recognizable in the constituent cells (Fig. 6-1e, 1f). CXCR4 and CXCL12 were recognizable on a few constituent cells, respectively (Fig. 6-1e, 1-f).

In the section of the spots from the AH rats, CXCR4 was recognizable mainly on the cell membrane of the AH7974 cells and partly on the cell membrane of the endothelial cells and blood cells (Fig. 6-2b). In addition, CXCL12 was recognizable in blood endothelial cells (Fig. 6-2c).

Transmission electron microscopy findings of milky spots

Mesothelial cells were visible on the surface of milky spots from the CONT rats that were observed in the TEM photographs (Fig. 7a). Various cells, including macrophages, lymphocytes, eosinophils, mast cells, and plasma cells, and blood vessels were seen under the mesothelial cells (Fig. 7a). Macrophages were present between the methothelial cells (Fig. 7b).

An invasion of AH7974 cells were clearly visible in the milky spots of the AH group (Fig. 7c). There were contact images of mast cells and eosinophils (Fig. 7d). Cell division images of the endothelial cells were also found in the spots (Fig. 7e).

Fluorescence microscopic analysis of GFP-tagged AH7974 cells

Green fluorescence protein-tagged AH7974 cells cultured in RPMI1640 medium with 20% FBS primarily showed fluorescence in the cytoplasm (Fig. 8b).

Auto-fluorescence of the red blood cell and the eosinophils was observed in the milky spots from the CONT rats (data not shown).

The fluorescence of the GFP-tagged AH7974 cells in the spots from the AH rats was shown to be in the outer layer of the milky spot. The presence of fluorescence-positive

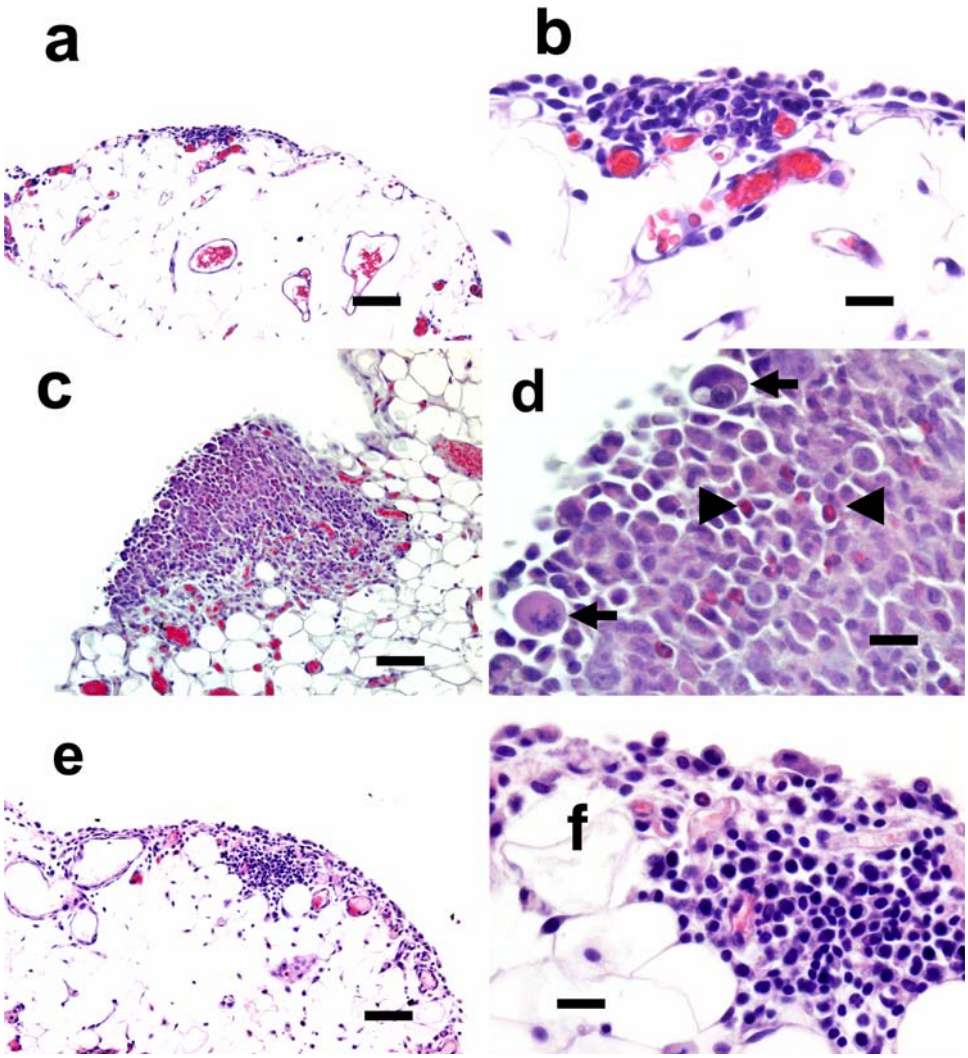

Fig. 5 Histological analysis of the milky spot. Paraffin sections from CONT (**a**, **b**), AH (**c**, **d**), and AMD (**e**, **f**) rats were stained with hematoxylin and eosin. Many cell types and blood vessels are seen in all sections and, in particular, the number of cells and vessels are increased in the section from the AH rats. *Arrows* AH7974 cells, *arrowheads* show eosinophils (**d**). *Scale bars*: 50 μm (**a**, **c**, **e**), 20 μm (**b**, **d**, **f**)

AH7974 cells was noted in some of the blood vessels (arrow), and the autofluorescence signal was recognized on the erythrocytes in the blood vessels (Fig. 8d).

A few GFP-tagged AH7974 cells were recognizable in the spots from the AMD rats, but these were fewer in number relative to the AH rats (Fig. 8f).

Discussion

The milky spot is the first site of implantation when cancer cells move into the peritoneal cavity. Yasumoto et al. (2006) definitively demonstrated that CXCR4 and CXCL12 play an important role in the metastasis of gastric cancer cells into the peritoneal cavity. However, the question of why a cancer cell first metastasizes to the milky spot on the omentum has not yet been answered. We therefore examined the role of CXCR4 and CXCL12 in the metastasis of the cancer cells into the milky spot.

We observed that the omentum was closely related to tumor metastasis, which supports the findings reported by Lawrance et al. (1991). We also found many number of blood vessels per area in the milky spots of the AH rats. One possible explanation is that these blood vessels are necessary for the metastasis and growth of the tumor cells. Images of an endothelial cell dividing in the milky spot and an increased number of blood vessels were also observed, possble suggestive of angiogenesis.

The number of eosinophils in milky spots from the AH rats increased in situ, but this is a new finding that has not yet been reported in earlier studies. Mast cells and eosinophils were in contact with each other in the milky spot of AH rats. It is possible that the eosinophil and mast cell are linked to the process of angiogenesis, but this was beyond the scope of our study. Further study is necessary to clarify this possible association.

The invasion of the AH7974 cells into the milky spot was examined using GFP fluorescence. In the spots from

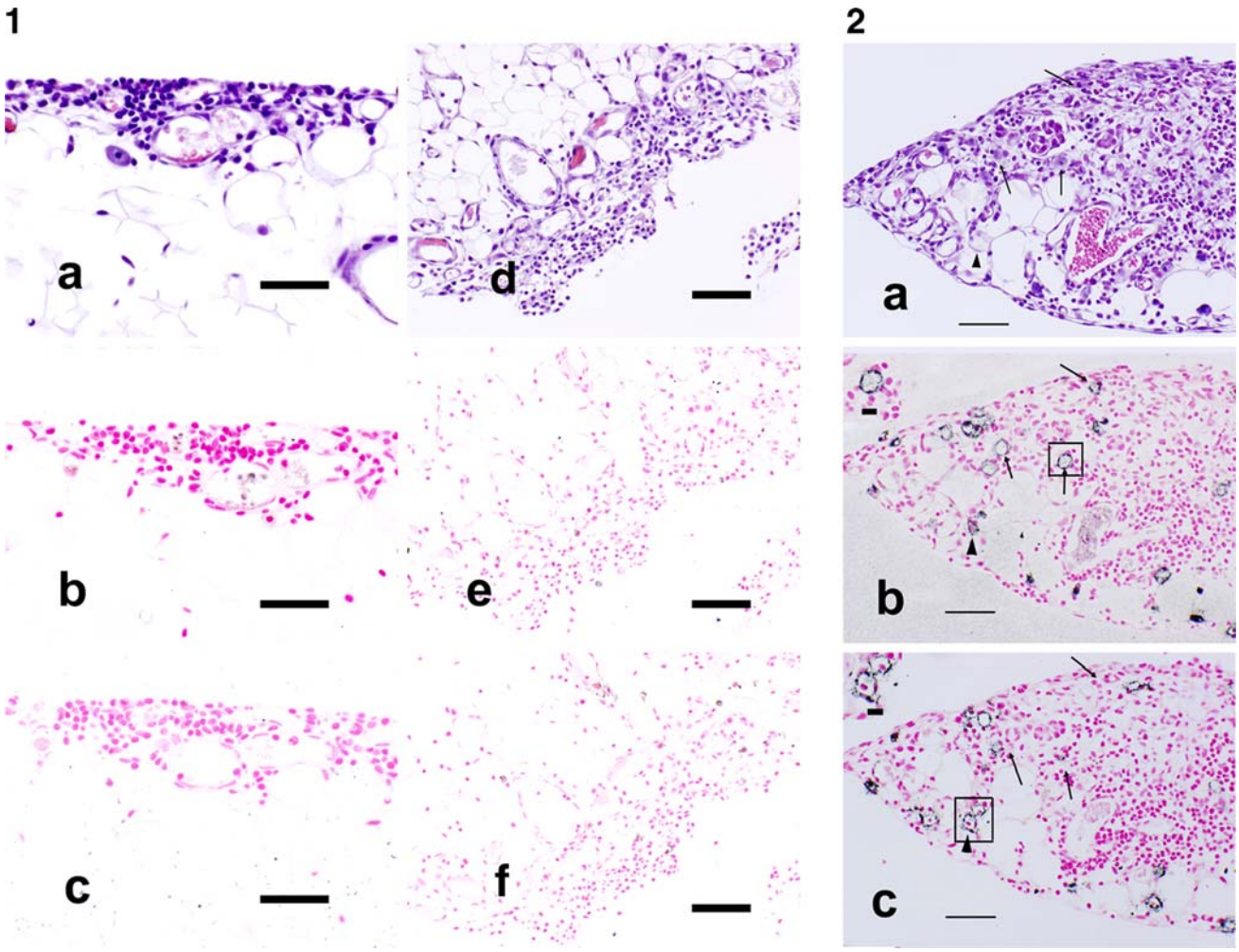

Fig. 6 Paraffin sections of milky spots stained with hematoxylin and eosin from the CONT (**1a**), AMD (**1d**), and AH (**2a**) rats. All of the serial sections are immunostained with anti-CXCR4 (**1b**, **1e**, **2b**) and anti-CXCL12 (**1c**, **1f**, **2c**) antibodies, respectively. **1b** CXCR4 was recognized on the red blood cells. **1c** CXCL12 protein was not recognized on the red blood cells. **1e** CXCR4 was recognized in a few constituent cells. **1f** CXCL12 was recognized in a few cells. **2b** CXCR4 was recognized on the cell membrane of the AH7974 cell (*arrows*); *inset* high magnification of the *arrowed* cell in the *square*. **2c** CXCL12 was recognized in blood endothelial cells; *enlarged image* is shown as the *inset*. *Squares* Tumor cell (**2b**) and a blood vessel (**2c**) as the *inset*. *Three arrows* in each figure indicate the same AH7974 cells. *Arrowheads* show the same blood vessel. *Scale bars*: 30 μm (**1a–c**), 50 μm (**1d–f**), 40 μm (**2a–c**), 10 μm (*inset*)

the AH rats, the fluorescence of the GFP-tagged AH7974 cells was shown in the outer layer of the milky spot and also in the blood vessels. This finding may imply metastasis via the blood stream. Although the tumor cells, which entered by an intravenous route, seemed to metastasize to the lung and liver, we were unable to confirm this process in our tissue specimens.

CXCL12 were not recognized in any of the cells of the milky spot from the CONT rats; however, CXCR4 was recognized on and in the some red blood cells. In the section of the spot from the AH rat, CXCL12 was recognized in the endothelial cells, while CXCR4 was recognized at the cell membrane of the AH7974 cells. CXCR4 and CXCL12 may therefore be related to each other as a keyhole and a key. An interesting observation was that CXCL12 was present in the milky spot from the AH rats but not in that from the CONT rats. Inoculation of the cancer cells into the abdominal cavity may have activated the endothelial cells of the milky spots, and we consider that these cells did produce CXCL12, possibly for guiding the tumor cells expressing CXCR4 into the blood vessels. One question has arisen. Why do the cancer cells invade the milky spots at the early stage of the transplantation of the cells to the peritoneal cavity? One possible answer is that this may be a function of the stomata, which have been described in the milky spots. The milky spot lacks a continuous basement membrane because of the presence of many pores, and it is different from other types of mesothelial tissue (Yonemura et al. 1996). It would seem that cancer cells are able to enter milky spot tissue

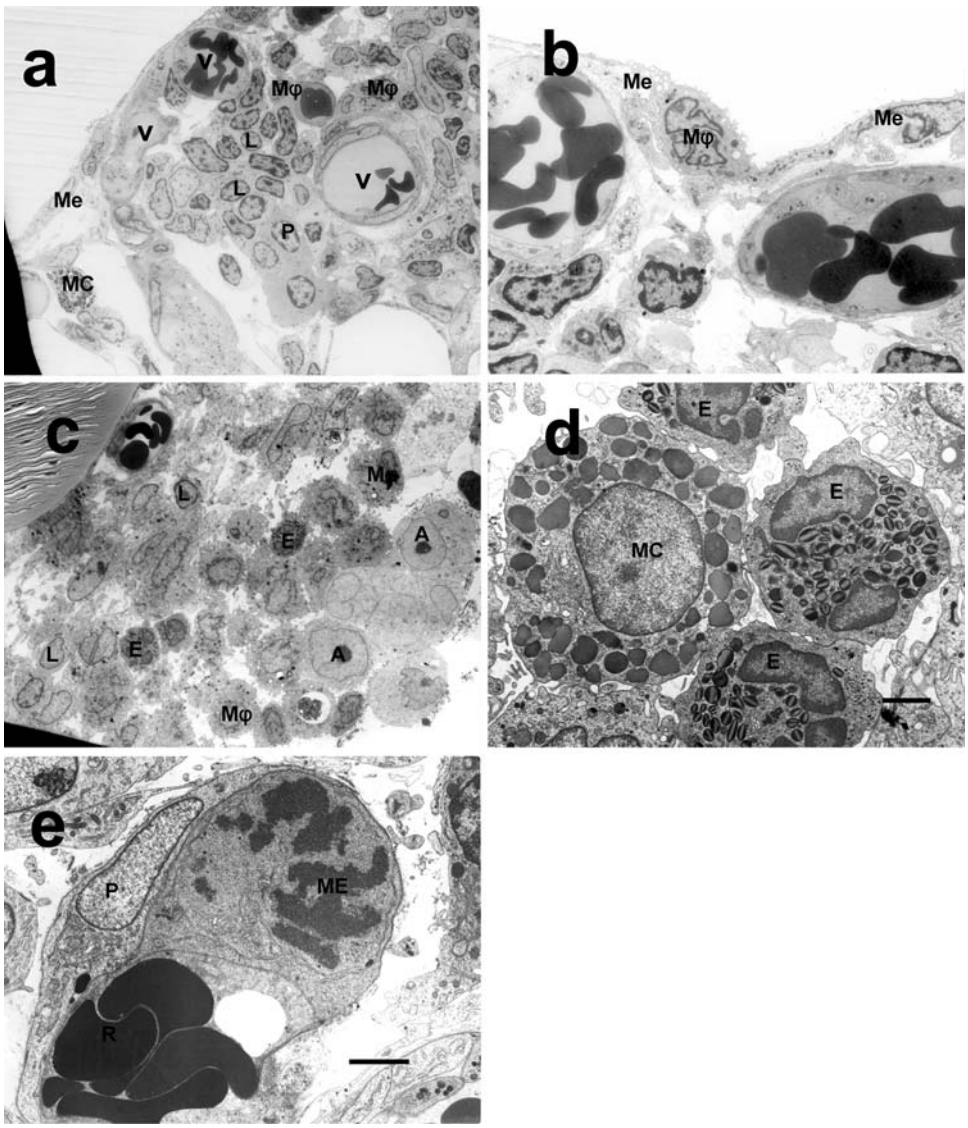

Fig. 7 Transmission electron microscopy analysis of the milky spots. **a**, **b** A milky spot of the CONT rats, **c**–**e** a milky spot of the AH rats. **a** Many kinds of cells are seen beneath the mesothelial cell layer. **b** Macrophages are present between the mesothelial cells. **c** AH7974 cells are recognized in the milky spot. **d** Contact image of a mast cell and eosinophils are seen. **e** Mitosis of an endothelial cell is recognized. *Scale bars*: 10 μm (**a**, **c**), 2 μm (**b**, **d**, **e**). *Me* mesothelial cell, *Mφ* macroghage, *L* lymphocyte, *P* plasma cell, *Mc* mast cell, *A* AH7974 cell, *E* eosinophil, *ME* mitotic endothelial cell, *P* pericyte, *R* red blood cell, *V* vein

simply because there are many pores at the surface of the milky spots.

Collectively, these results strongly suggest that CXCR4-expressing AH7974 cells are preferentially attracted to the surface of milky spots where its ligand CXCL12 is abundantly produced. In addition, the migration of cancer cells, their local growth, and/or survival are also important for cancer metastasis. CXCL12 is produced by several tumors, including ovarian cancer (Scotton et al. 2002) and pancreatic cancer (Koshiba et al. 2000) and is also produced by stromal cells, such as peritoneal mesothelial cells (Oonakahara et al. 2004; Sako et al. 2004), vascular endothelial cells, and fibroblasts. In particular, carcinoma-associated stromal fibroblasts have the capacity to efficiently secrete CXCL12 and promote tumor growth through an elevated secretion of CXCL12 (Orimo et al. 2005). Moreover, the interaction between VEGF, CXCR4, and CXCL12 has been recently reported to be relevant to the development of peritoneal metastasis (Bachelder et al. 2002; Kryczek et al. 2005). As such,the relations between VEGF, CXCR4, and CXCL12 need further analysis.

AMD3100 is a specific inhibitor of CXCR4 that plays an important role in the CXCL12/CXCR4 interaction in the milky spots of ascitic-type hepatoma bearing rats. The inhibition of the experimental peritoneal carcinomatosis induced by AMD3100 in our study was clearly shown by the reduced size of the milky spots in the AMD rats in comparison to that seen 3 days after the AH7974 cells were transplanted into the peritoneal cavity. A few GFP-tagged AH7974 cells were recognized in the spots from the AMD rats, but they were much fewer in number than what was observed in spots from AH rats. AMD3100 may be accustomed to the drug used for the control of metastasis of cancer-bearing patients.

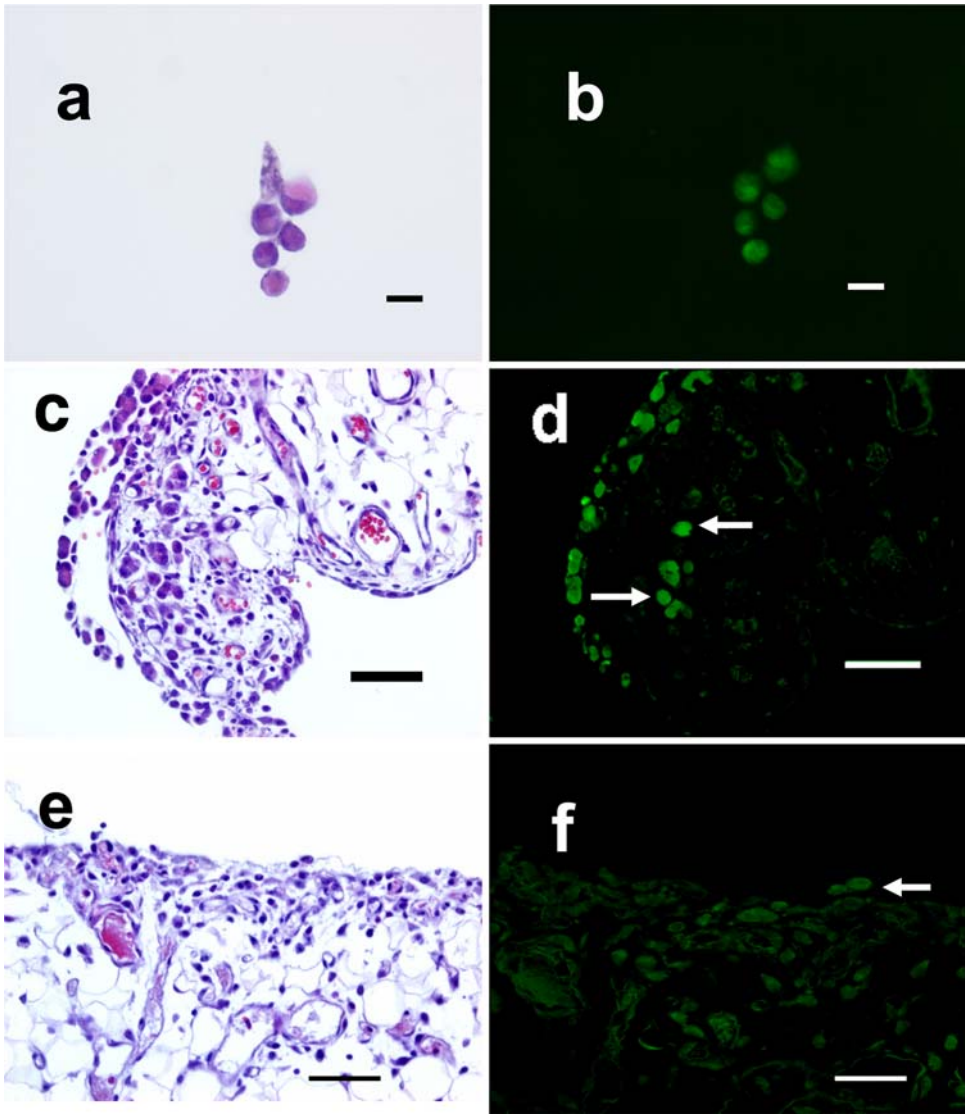

Fig. 8 Light and fluorescence microscopic analysis of green fluorescence protein (GFP)-tagged AH7974 cells and the milky spot. **a**, **b** Cultured GFP-tagged AH7974 cells were confirmed in the fluorescing milky spot. **c**, **d** A milky spot from an AH rat. GFP-tagged AH7974 cells are recognized at the outer layer of the milky spot and the tumor cells were rarely recognizable in the blood vessels (*arrows*). **e**, **f** A milky spot from an AMD rat. Fluorescence-positive AH7974 cells are only rarely visible (*arrow*). *Scale bars*: 10 μm (**a**, **b**), 50 μm (**c**, **d**), 30 μm (**e**, **f**)

Based on our results, we suggest that AH7974 cells initially invade into the milky spots for the following reasons: (1) since CXCL12 was abundantly present on the vascular walls in the milky spots from the AH rats, and the AH7974 cells expressed its receptor CXCR4, AH7974 cells would likely migrate toward the milky spots; (2) there were abundant blood vessels in the milky spots which were necessary for the survival, growth, and metastasis of the tumor cells; (3) the peritoneal cavity is covered with a mono-layer of mesothelial cells that lack a basement membrane in the basal surface, but pores were observed between the neighboring mesothelial cells on the surface of the milky spots. The tumor cells have difficulty invading the mesothelial layer without pores. However, the tumor cells easily invade the peritoneum, which has pores and lacks a basement membrane.

In conclusion, we may be able to say that (1) both CXCR4 and CXCL12 molecules participate in the invasion of the tumor cells to the milky spots; (2) AMD3100 acts as an inhibitor of tumor cell entry to the milky spots.

Acknowledgments We thank Dr. Nobuoki Eshima (Oita University School of Medicine) for his informative advice on the manuscript, and Dr. Noritaka Matsuo (Oita University School of Medicine) for his helpful comments and suggestions on our study.

References

Bachelder RE, Wendt MA, Mercurio AM (2002) Vascular endothelial growth factor promotes breast carcinoma invasion in an autocrine manner by regulating the chemokine receptor CXCR4. Cancer Res 62:7203–7206

Bleul CC, Farzan M, Choe H et al (1996) The lymphocyte chemoattractant SDF-1 is a ligand for LESTR/fusin and blocks HIV-1 entry. Nature 382:829–833

Clercq ED, Yamamoto N, Pauwels R et al (1992) Potent and selective inhibition of human immuno-deficiency virus (HIV-1) and HIV-

2 replication by a class of bicyclams interacting with a viral uncoating event. Proc Natl Acad Sci USA 89:5286–5290
Clercq ED, Yamamoto N, Pauwels R et al (1994) Highly potent and selective inhibition of human immunodeficiency virus by the bicyclam derivative JM3100. Antimicrob Agents Chemother 38:668–674
Egawa T, Kawabata K, Kawamoto H et al (2001) The earliest stages of B cell development require a chemokine stromal cell-derived factor/pre-B cell growth-stimulating factor. Immunity 15:323–334
Feng Y, Broder CC, Kennedy PE, Berger EA (1996) HIV-1 entry cofactor: functional cDNA cloning of a seven-transmembrane, G protein-coupled receptor. Science 272:872–877
Geminder H, Sagi-Assif O, Goldberg L et al (2001) A possible role for CXCR4 and its ligand, the CXC chemokine stromal cell-derived factor-1, in the development of bone marrow metastases in neuroblastoma. J Immunol 167:4747–4757
Green J, Williams AE (1978) The relationship between inflammatory responses and WBP1 tumour cell attachment to the rat omentum. Eur J Cancer 14:1153–1155
Higgins GM, Bain CG (1930) The absorption and transference of particulate material by the great omentum. Surg Gynecol Obstet 50:851–860
Jones D, Benjamin RJ, Shahsafaei A, Dorfman DM (2000) The chemokine receptor CXCR3 is expressed in a subset of B-cell lymphomas and is a marker of B-cell chronic lymphocytic leukemia. Blood 95:627–632
Kato S, Miura M, Miyauchi R (1993) Enzyme-histochemical staining method for lymphatics and blood capillaries. Jpn J Lymphol 16:9–17
Kitamura H, Nagai K, Nakamura M (1991) Improvement of a physical developer devoid of gum Arabic for immunohistochemical use. Acta Histochem Cytochem 24:521
Koshiba T, Hosotani R, Miyamoto Y et al (2000) Expression of stromal cell-derived factor 1 and CXCR4 ligand receptor system in pancreatic cancer: a possible role for tumor progression. Clin Cancer Res 6:3530–3535
Krist LFG, Eestermans IL, Steenbergen JJE et al (1995) Cellular composition of milky spots in the human greater omentum: an immuno-chemical and ultrastructural study. Anat Rec 241:163–174
Kryczek I, Lange A, Mottram P et al (2005) CXCL12 and vascular endothelial growth factor synergistically induce neoangiogenesis in human ovarian cancers. Cancer Res 65:465–472
Lawrance RJ, Loizidou M, Cooper AJ, Alexander P, Taylor I (1991) Importance of the omentum in the development of intra-abdominal metastases. Br J Surg 78:117–119
Mashino K, Sadanaga N, Yamaguchi H et al (2002) Expression of chemokine receptor CCR7 is associated with lymph node metastasis of gastric carcinoma. Cancer Res 62:2937–2941
Murphy PM (2001) Chemokines and the molecular basis of cancer metastasis. N Eng J Med 345:833–835
Nagasawa T, Kikutani H, Kishimoto T (1994) Molecular cloning and structure of a pre-B-cell growth-stimulating factor. Proc Natl Acad Sci USA 91:2305–2309
Nagasawa T, Tachibana K, Kawabata K (1999) A CXC chemokine SDF-1/PBSF a ligand for a HIV corecepter, CXCR4. Adv Immunol 71:211–228
Nanki T, Lipsky PE (2000) Cutting edge: Stromal cell-derived factor-1 is a co-stimulator for CD4+ T cell activation. J Immunol 164:5010–5014
Oberlin E, Amara A, Bachelerie F et al (1996) The CXC chemokine SDF-1 is the ligand for LESTER/fusin and prevents infection by T-cell-line-adapted HIV-1. Nature 382:833–835
Oonakahara K, Matsuyama W, Higashimoto I et al (2004) Stromal cell-derived factor-1α/CXCL12-CXCR4 axis is involved in the dissemination of NSCLC cells into pleural space. Am J Respir Cell Mol Biol 30:671–677
Orimo A, Gupta PB, Sgroi DC et al (2005) Stromal fibroblasts present in invasive human breast carcinomas promote tumor growth and angiogenesis through elevated SDF-1/CXCL12 secretion. Cell 121:335–348
Rempel SA, Dudas S, Ge S, Gutierrez JA (2000) Identification and localization of the cytokine SDF1 and its receptor, CXC chemokine receptor 4, to regions of necrosis and angiogenesis in human glioblastoma. Clin Cancer Res 6:102–111
Rossi D, Zlotnik A (2000) The biology of chemokines and their receptors. Annu Rev Immunol 18:217–242
Sako A, Kitayama J, Koyama H et al (2004) Transduction of soluble Flt-1 gene to peritoneal mesothelial cells can effectively suppress peritoneal metastasis of gastric cancer. Cancer Res 64:3624–3628
Scotton CJ, Wilson JL, Scott K et al (2002) Multiple actions of the chemokine CXCL12 on epithelial tumor cells in human ovarian cancer. Cancer Res 62:5930–5938
Seifert E (1921) Zur Biologie des menschlichen großen Netzes. Arch Klin Chir 116:510–517
Shimotsuma M, Takahashi T, Kawata M, Dux K (1991) Cellular subsets of the milky spots in the human greater omentum. Cell Tissue Res 264:599–601
Shimotsuma M, Margan MWS, Takahashi T, Hagiwara A (1992) Activation of omental milky spots and milky spot macrophages by intraperitoneal administration of a streptococcal preparation, OK-432. Cancer Res 52:5400–5402
Shiomi K, Miyamoto H, Segawa T et al (2006) Novel ELISA system for detection of N-ERC/mesothelin in the sera of mesothelioma patients. Cancer Sci 97:928–932
Strieter RM (2001) Chemokines: not just leukocyte chemoattractants in the promotion of cancer. Nat Immunol 2:285–286
Taichman RS, Cooper C, Keller ET, Pienta KJ, Taichman NS, McCauley LK (2002) Use of the stromal cell-derived factor-1/CXCR4 pathway in prostate cancer metastasis to bone. Cancer Res 62:1832–1837
Vreese KD, Kofler-Mongold V, Leutgeb C et al (1996a) The molecular target of bicyclams, potent inhibitors of human immunodeficiency virus replication. J Virol 70:689–696
Vreese KD, Reymen D, Griffin P et al (1996b) The bicyclams, a new class of potent human immunodeficiency virus inhibitors, block viral entry after binding. Antiviral Res 29:209–219
Yasumoto K, Koizumi K, Kawashima A et al (2006) Role of the CXCL12/CXCR4 axis in peritoneal carcinomatosis of gastric cancer. Cancer Res 66:2181–2187
Yonemura Y, Endo Y, Yamaguchi T et al (1996) Mechanisms of the formation of the peritoneal dissemination in gastric cancer. Int J Oncol 8:795–802
Yoshida T (1971) Comparative studies of ascites hepatomas. Methods Cancer Res 6:97–157
Yoshie O, Imai T, Nomiyama H (1997) Novel lymphocyte-specific CC chemokines and their receptors. J Leukoc Biol 62:634–644